Influence of electron-phonon interaction on spin-fluctuation-induced superconductivity

T. S. Nunner*

Institut für Theoretische Physik, Freie Universität Berlin, Arnimallee 14, D-14195 Berlin, Germany

J. Schmalian

Department of Physics, University of Illinois at Urbana-Champaign, Urbana, Illinois 61801
and Institut für Theoretische Physik, Freie Universität Berlin, Arnimallee 14, D-14195 Berlin, Germany

K. H. Bennemann

Institut für Theoretische Physik, Freie Universität Berlin, Arnimallee 14, D-14195 Berlin, Germany

We investigate the interplay of the electron-phonon and the spin-fluctuation interaction in the superconducting state of $YBa_2Cu_3O_7$. The spin fluctuations are described within the nearly antiferromagnetic Fermi-liquid theory and the phonons are treated using a shell-model calculation of all phonon branches. The electron-phonon coupling is calculated using rigidly displaced ionic potentials screened by a background dielectric constant ε_∞ and by holes within the CuO_2 planes. We get a superconducting state with $d_{x^2-y^2}$ symmetry whose origin is antiferromagnetic spin fluctuations. The phononic contribution of *all* phonon modes of the system to the d-wave pairing interaction is attractive. This gives a positive isotope effect. The size of the isotope exponent depends strongly on the relative strength of the electron-phonon and spin-fluctuation coupling. Due to the strong electronic correlations no phononic induced superconducting state of s-wave character, is possible. [S0163-1829(99)02713-7]

I. INTRODUCTION

The mechanism responsible for the superconducting state of high-T_c superconductors is still discussed highly intensively. Cooper pairing induced by spin fluctuations[1–3] seems to be likely. Based on the analysis of NMR experiments,[4] it offers an explanation for transport and optical experiments[5(a)] and a variety of anomalies in underdoped cuprates[6,7] and furthermore yields a $d_{x^2-y^2}$-wave pairing state with a transition temperature T_c of correct order of magnitude.[8]

However, there are also observations, which indicate effects due to the electron-phonon interaction. Raman-scattering experiments and IR measurements show the softening of some phonon modes as the temperature is decreased below T_c.[9,10] In $YBa_2Cu_3O_7$ the largest shift was found for the 340 cm^{-1} (42 meV) Raman-active mode of B_{1g} symmetry, which involves the out-of-plane vibration of the oxygen atoms O(II) and O(III) in the copper-oxygen planes.[11] For some oxygen-related phonon modes the onset of the frequency softening was found to start even 50–60 K above T_c.[12] The temperature dependence of this anomaly was found to be similar to that of the NMR relaxation rate $(T_1 T)^{-1}$, which, in the latter case, is due to an anomalous behavior of the spin excitations, and indicates a possible coupling between phonons and spin degrees of freedom.[12] Especially interesting is the observation of the anomalous oxygen isotope effect in the high-T_c superconductors.[13] At optimal doping with largest T_c only a very small oxygen isotope exponent $\alpha = 0 - 0.07$ is observed, whereas in the underdoped and overdoped systems the isotope exponent can reach values close to the BCS value $\alpha = \frac{1}{2}$.

Due to these experimental findings it is of interest to investigate in more detail the influence of electron-phonon in-

teraction on the spin-fluctuation-induced superconducting state. In this context it was shown that oxygen buckling modes support a $d_{x^2-y^2}$-pairing state, whereas oxygen breathing modes will support an s-wave state.[14–16] Hence, an analysis of the role of the electron-phonon interaction in the cuprates has to take into account all vibrational modes.

In this paper we investigate the interplay of the spin fluctuation and the electron-phonon interaction in the superconducting state of $YBa_2Cu_3O_7$. We find that taking into account both the spin fluctuation and electron-phonon interaction gives a superconducting state of $d_{x^2-y^2}$ symmetry, while the electron-phonon interaction alone would yield an anisotropic s-wave pairing with a much smaller critical temperature. The $d_{x^2-y^2}$-superconducting state is caused by antiferromagnetic spin fluctuations and the critical temperature T_c is reduced by simultaneous consideration of phonons. Nevertheless we find a positive isotope effect. We show that the momentum dependence of the total electron-phonon interaction amplifies the pairing interaction by an amount of about 5–10% in the $d_{x^2-y^2}$-wave channel, which is a necessary condition for a positive isotope effect. Furthermore we identify the phonon modes, which make the most dominant contribution to the $d_{x^2-y^2}$-pairing interaction. The decrease of T_c is explained by the large isotropic part of the electron-phonon interaction, which enhances the electron scattering rate significantly. However, this effect will be reduced when correlation-effects are taken into account, since correlation induced suppression of charge fluctuations will predominantly reduce the isotropic part of the electron-phonon interaction. Our results are obtained with a self-consistent strong-coupling Eliashberg calculation. Finally, in order to make this interplay of the spin fluctuation and electron-phonon in-

teraction more transparent, we present a simple weak-coupling model.

In the present work we will not address a variety of rather important aspects of the electron-phonon interaction in cuprates. In calculating the electron-phonon coupling constants, we will completely ignore the correlated nature of the involved charge carriers, even though this is expected to be essential to deduce reliable quantitative information about the strength of this interaction and its relative importance for different phonon modes. Based on calculations by Zeyher and Kulić,[17] we can at least show that the latter aspect does not oppose the conclusions of our results. Furthermore, lattice anharmonicities will also be neglected, since we believe that within the presented framework, where the mutual influence of electron-phonon and spin-fluctuation interaction is investigated within an Eliashberg theory, anharmonicities, if relevant for the cuprates at all, can hardly affect our result. These rather drastic approximations are necessary to enable us to draw quantitative, material specific conclusions about the role of phonons within a spin-fluctuation scenario. The main complication in this context is that, in distinction to the electronic system, the phononic degrees of freedom behave completely three dimensional, and there is no obvious restriction to a few relevant phonon modes.

II. THEORY

The coupled electron-phonon system is characterized by the Hamiltonian:

$$H = \sum_{\mathbf{k}\sigma} \varepsilon_{\mathbf{k}} c^{\dagger}_{\mathbf{k},\sigma} c_{\mathbf{k},\sigma} + g_{\mathrm{sf}} \sum_{\mathbf{k}\mathbf{q}\sigma\sigma'} c^{\dagger}_{\mathbf{k},\sigma} \vec{\sigma}_{\sigma,\sigma'} c_{\mathbf{k}+\mathbf{q},\sigma'} \cdot \vec{S}_{-\mathbf{q}}$$

$$+ \sum_{\mathbf{k},\mathbf{q}\lambda\sigma} g_{\lambda}(\mathbf{q}) c^{\dagger}_{\mathbf{k},\sigma} c_{\mathbf{k}+\mathbf{q},\sigma}(b^{\dagger}_{\mathbf{q},\lambda} + b_{\mathbf{q},\lambda})$$

$$+ \sum_{\mathbf{q}\lambda} \omega_{\mathbf{q},\lambda} b^{\dagger}_{\mathbf{q},\lambda} b_{\mathbf{q},\lambda}. \qquad (1)$$

Here, $c^{\dagger}_{\mathbf{k}\sigma}$ is the electron creation operator of the hybridized Cu-3$d_{x^2-y^2}$ and O-2$p_{x,y}$ orbitals with energy $\varepsilon_{\mathbf{k}}$ describing the fermionic low-energy degrees of freedom.[19] The spin fluctuations are treated in terms of the interaction of the electron spin with a spin-field $\vec{S}_{\mathbf{q}}$ characterized by a spin susceptibility $\chi(\mathbf{q},\omega)$. Note, alternatively one could also use a Hubbard-like Hamiltonian and determine $\chi(\mathbf{q},\omega)$ diagrammatically, e.g., within the fluctuation exchange approximation,[18] which would not change the conclusions of this paper. The present method has the advantage that $\chi(\mathbf{q},\omega)$ can be chosen in agreement with the experimentally observed spin susceptibility of YBa$_2$Cu$_3$O$_7$. In Eq. (1) $b^{\dagger}_{\mathbf{q}\lambda}$ is the creation operator of a phonon in the vibrational branch λ with energy $\omega_{\mathbf{q},\lambda}$ and $g_{\lambda}(\mathbf{q})$ is the electron-phonon coupling constant of the λth phonon branch with the above Cu-O hybrid states. For the electronic band dispersion we use

$$\epsilon(\mathbf{k}) = -2t(\cos k_x + \cos k_y) - 4t'\cos k_x \cos k_y, \qquad (2)$$

with the nearest-neighbor hopping $t = 250$ meV and the next-nearest-neighbor hopping $t' = -0.45t$, which reproduce the bandwidth and Fermi-surface shape of YBa$_2$Cu$_3$O$_7$.

The short-ranged antiferromagnetic spin fluctuations are described within the nearly antiferromagnetic Fermi-liquid approach by the dynamical spin susceptibility:[4]

$$\mathrm{Im}\,\chi(\mathbf{q},\omega) = \mathrm{Im}\left(\frac{\chi_Q}{1 + \xi^2(\mathbf{Q}-\mathbf{q})^2 - i\omega/\omega_{\mathrm{sf}}}\right). \qquad (3)$$

Here, values for the antiferromagnetic correlation length $\xi = 2.3a$, the spin-fluctuation energy $\omega_{\mathrm{sf}} = 14$ meV and $\chi_Q = 75$ meV are chosen as in Ref. 8, which are deduced from the analysis of NMR and NQR experiments of YBa$_2$Cu$_3$O$_7$. The resulting pairing interaction of the spin-fluctuation interaction is given by

$$V^{\mathrm{sf}}_{\mathbf{q}}(\omega) = g^2_{\mathrm{sf}}\chi(\mathbf{q},\omega). \qquad (4)$$

The electron-spin fluctuation coupling constant $g_{\mathrm{sf}} = 0.68$ eV for an electron concentration of $n_e = 0.8$ is chosen as in Ref. 8, which was shown to yield $T_c = 90$ K and quantitative agreement with transport experiments, if one assumes that these are entirely due to spin fluctuations.[5(a)]

The phonons are described within a shell model, where the dynamical matrix is obtained from the derivative of the lattice potential, which consists of Coulomb potentials with core and shell charges, Born-Mayer repulsive potentials, and core-shell polarizabilities. Details of the calculation are the same as in Ref. 20. For the description of YBa$_2$Cu$_3$O$_7$ we use parameters, for the core and shell charges, Born-Mayer parameters, and polarizabilities as given in Ref. 21. The shell model was shown to give excellent agreement with experimentally determined phonon dispersion curves for several cuprate systems and is based on a rather small set of physically well motivated parameters. The corresponding electron-phonon coupling is calculated using a model recently proposed by Zeyher,[22] which uses rigidly displaced ionic potentials screened by a dielectric constant ϵ_{∞} and by holes within the CuO$_2$ planes. We have modified this model to allow for the explicit consideration of local field corrections taking the relative position of the screening CuO$_2$ planes and the vibrating ions explicitly into account. The coupling of the phonon-mode λ to an electron localized at the site κ within the primitive cell is given by

$$g_{\kappa\lambda}(\mathbf{q}) = -\sum_{\kappa'\alpha} \frac{Z_{\kappa'}e^2}{v_c^{2/3}} \sqrt{\frac{\hbar}{2\omega_{\lambda}(\mathbf{q})}} \left(\frac{e_{\alpha\kappa'\lambda}(\mathbf{q})}{\sqrt{M_{\kappa'}}} \Phi^{(2)}_{\kappa\kappa'\alpha}(\mathbf{q}) \right.$$

$$\left. - \frac{e_{\alpha\kappa\lambda}(\mathbf{q})}{\sqrt{M_{\kappa}}} \Phi^{(1)}_{\kappa\kappa'\alpha}(0) \right). \qquad (5)$$

M_{κ} and Z_{κ} are the mass and the charge of the ion with basis index κ, v_c is the volume of the primitive cell, $\omega_{\lambda}(\mathbf{q})$ and $e_{\alpha\kappa\lambda}$ are the vibration frequency and the normalized eigenvector of the phonon mode λ with wave vector $\mathbf{q}$, and α is a Cartesian index. $\Phi^{[1(2)]}_{\kappa\kappa'\alpha}$ denotes the contribution of the κ' ion to the total Coulomb potential at lattice site κ, which is caused by the vibration of the ion κ' and of the ion κ, respectively:

$$\Phi_{\kappa\kappa'\alpha}^{[1(2)]}(\mathbf{q}) = \frac{i}{v_c^{1/3}} \sum_{\mathbf{G_1G_2}} \epsilon^{-1}(\mathbf{k+G_1,k+G_2}) v(\mathbf{k+G_2})$$

$$\times (\mathbf{k+G_{1(2)}})_\alpha e^{i\mathbf{G_1}\kappa} e^{-i\mathbf{G_2}\kappa'}. \qquad (6)$$

$\mathbf{G_1,G_2}$ are reciprocal-lattice vectors and $v(\mathbf{k}) = e^2/\epsilon_0 \mathbf{k}^2$ denotes the bare Coulomb interaction. The inverse dielectric function ϵ^{-1} will be discussed in the Appendix.

For simplicity we assume, that the Cooper pair forming electrons are mainly located at the in-plane Cu sites. Therefore, only the coupling $g_{\kappa\lambda}$ where κ refers to the Cu(II) site will be considered. This index κ can be suppressed in the following. The electron-phonon induced pairing interaction is given by

$$V_{\mathbf{q}}^{\mathrm{ph}}(i\omega_n) = \frac{1}{N_z} \sum_{q_z,\lambda} g_\lambda(\mathbf{q},q_z)^2 \frac{2\omega_{\mathbf{q},q_z,\lambda}}{(i\omega_n)^2 - \omega_{\mathbf{q},q_z,\lambda}^2}. \qquad (7)$$

Here, the summation with respect to q_z takes into account that the pairing interaction can also be generated by phonons propagating perpendicular to the $\mathrm{CuO_2}$ planes, even if the paired electrons are within these planes.

The total electron-phonon coupling strength may then be characterized, e.g., via the dimensionless parameter

$$\lambda = 2 \int_0^\infty \frac{\alpha^2 F(\omega)}{\omega} d\omega, \qquad (8)$$

where the McMillan function $\alpha^2 F$ is defined by

$$\alpha^2 F(\omega) = \frac{1}{\displaystyle\sum_{\mathbf{k}} \delta(\epsilon_{\mathbf{k}})} \sum_{\mathbf{kk'}} \delta(\epsilon_{\mathbf{k}}) \delta(\epsilon_{\mathbf{k'}})$$

$$\times \sum_\lambda |g(\mathbf{k,k'},\lambda)|^2 \delta(\omega - \omega_\lambda(\mathbf{k-k'})). \qquad (9)$$

Having discussed the spin-fluctuation and electron-phonon induced interactions, we investigate the superconducting state within the strong-coupling Eliashberg theory, where as usual, the self energy is expanded with respect to unitary and Pauli matrices in Nambu space $\hat{\tau}^i$:

$$\hat{\Sigma}_{\mathbf{k}}(i\omega_n) = Y_{\mathbf{k}}(i\omega_n)\hat{\tau}^0 + X_{\mathbf{k}}(i\omega_n)\hat{\tau}^3 + \Phi_{\mathbf{k}}(i\omega_n)\hat{\tau}^1 \ . \qquad (10)$$

$Y_{\mathbf{k}}(i\omega_n) = i\omega_n[1 - Z_{\mathbf{k}}(i\omega_n)]$ and $X_{\mathbf{k}}(i\omega_n)$ refer to the self-energy renormalizations which occur also in the normal state and $\Phi_{\mathbf{k}}(i\omega_n) = \Delta_{\mathbf{k}}(i\omega_n) Z_{\mathbf{k}}(i\omega_n)$ to the anomalous self-energy which is nonzero only in the superconducting state. $\omega_n = (2n+1)\pi/\beta$ are the fermionic Matsubara frequencies, with $\beta = 1/T$. The self-energies are determined by the Eliashberg equations:

$$\Phi_{\mathbf{k}}(i\omega_n) = \frac{1}{\beta} \sum_{\mathbf{k'},n'} \frac{[\tilde{V}_{\mathbf{k,k'}}(i\omega_n - i\omega_{n'})]\Phi_{\mathbf{k'}}(i\omega_{n'})}{D_{\mathbf{k'}}(i\omega_{n'})},$$

$$X_{\mathbf{k}}(i\omega_n) = \frac{1}{\beta} \sum_{\mathbf{k'},n'} \frac{V_{\mathbf{k,k'}}(i\omega_n - i\omega_{n'})[\epsilon_{\mathbf{k'}} + X_{\mathbf{k'}}(i\omega_{n'})]}{D_{\mathbf{k'},\lambda'}(i\omega_{n'})},$$
$$(11)$$

$$Y_{\mathbf{k}}(i\omega_n) = \frac{1}{\beta} \sum_{\mathbf{k'},n'} \frac{V_{\mathbf{k,k'}}(i\omega_n - i\omega_{n'}) i\omega_{n'} Z_{\mathbf{k'}}(i\omega_{n'})}{D_{\mathbf{k'}}(i\omega_{n'})},$$

where

$$\tilde{V}_{\mathbf{k,k'}}(i\omega_n) = V_{\mathbf{k-k'}}^{\mathrm{sf}}(i\omega_n) + V_{\mathbf{k-k'}}^{\mathrm{ph}}(i\omega_n), \qquad (12)$$

$$V_{\mathbf{k,k'}}(i\omega_n) = V_{\mathbf{k-k'}}^{\mathrm{sf}}(i\omega_n) - V_{\mathbf{k-k'}}^{\mathrm{ph}}(i\omega_n), \qquad (13)$$

and the denominator is given by

$$D_{\mathbf{k'}}(i\omega_{n'}) = [i\omega_{n'}Z_{\mathbf{k'}}(i\omega_{n'})]^2$$
$$-[\epsilon_{\mathbf{k'}} + X_{\mathbf{k'}}(i\omega_{n'})]^2 - \Phi_{\mathbf{k'}}(i\omega_{n'})^2. \qquad (14)$$

After analytical continuation to the real frequency axis, $i\omega_n = i(2n+1)\pi/\beta \rightarrow \omega + i0^+$, this set of coupled equations is solved self-consistently using the numerical framework of Ref. 23. We do not restrict the momentum summation to the Fermi surface but take the entire Brillouin zone (BZ) into account. Since both pairing interactions V^{sf} and V^{ph} are chosen to reproduce the experimental spin susceptibility and phonon dispersion, we do not take additional renormalizations of $V_{\mathbf{q}}(i\omega_n)$ and $\tilde{V}_{\mathbf{q}}(i\omega_n)$ into account.

III. RESULTS

First, we will demonstrate that our treatment of the spin fluctuations yields indeed a superconducting state with $d_{x^2-y^2}$ symmetry and a reasonable critical temperature. The effective interaction due to spin fluctuations is repulsive for all momenta and is peaked at the antiferromagnetic wave vector $\mathbf{Q} = (\pi/a, \pi/a)$, as can be seen in Fig. 1. In agreement with Ref. 8, the self-consistent solution of the Eliashberg equations yields $d_{x^2-y^2}$ superconductivity, as can be deduced from the momentum dependence of the off-diagonal self-energy in Fig. 2(a), which exhibits the typical form: $\Phi \sim (\cos k_x - \cos k_y)$.

Variation of the temperature shows that the superconducting gap vanishes around 110 K. Although this is slightly larger than the experimental critical temperature of $\mathrm{YBa_2Cu_3O_7}$, we decided to accept this still reasonable value for T_c, since the spin-fluctuation interaction has already been chosen in agreement with transport experiments[5] and manipulation of the electron-spin-fluctuation coupling constants would introduce new and arbitrary parameters.

In the following we investigate the influence of the electron-phonon interaction on the spin-fluctuation-induced superconducting state. Solving the Eliashberg equations yields $d_{x^2-y^2}$ superconductivity even in the presence of phonons, as can be seen from the momentum dependence of the gap function in Fig. 2. For obtaining some information about the isotope effect, we have performed Eliashberg calculations for two different oxygen isotopes O(16) and O(18).
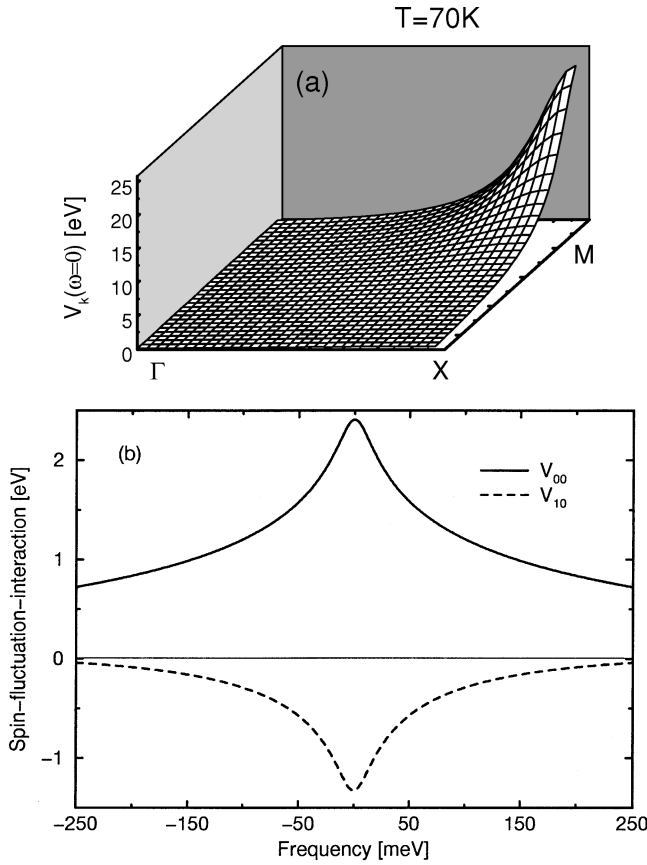
FIG. 1. Spin-fluctuation interaction at $T=70$ K: (a) momentum dependence of the spin-fluctuation interaction for frequency $\omega=0$, (b) frequency dependence of the on-site interaction V_{00} and the nearest-neighbor interaction V_{10}.
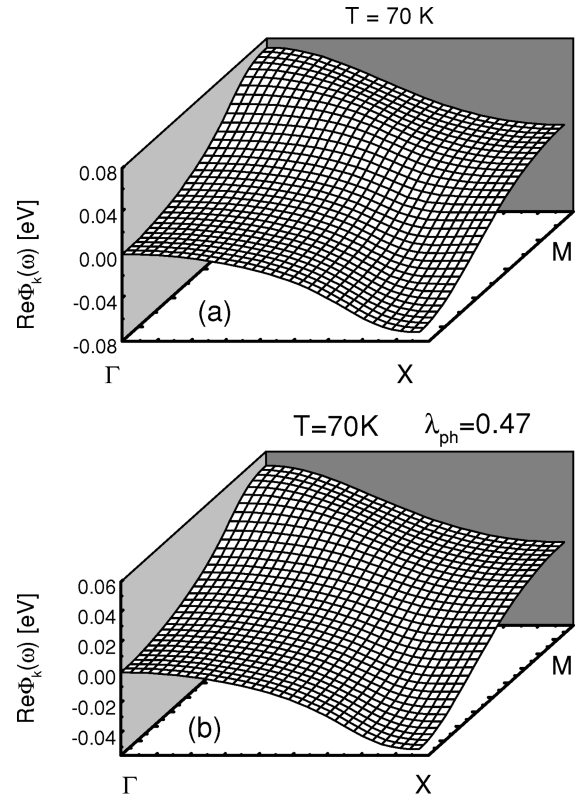

FIG. 2. Off-diagonal self-energy $\Phi_k(\omega)$ for (a) only spin-fluctuation induced superconductivity and (b) both phonon and spin fluctuation induced superconductivity. In both cases the superconducting state is characterized by $d_{x^2-y^2}$-symmetry order parameter, since $\Phi_k \sim (\cos k_x - \cos k_y)$. Note, $\Phi_k(\omega)$ is reduced due to the electron-phonon interaction.

For this the whole electron-phonon interaction, i.e., the phonon dispersions and the electron-phonon coupling constants, has been calculated separately for the two oxygen masses. In Fig. 3 the momentum-averaged density of states at a temperature of $T=80$ K is shown for the two oxygen isotopes O(16) and O(18). For comparison the density of states for only spin-fluctuation-induced superconductivity is shown as well. Two important things can be learned from Fig. 3: the superconducting gap is reduced dramatically in the presence of phonons, but nevertheless the isotope effect is positive. This can be inferred from the fact that there still remains a small superconducting gap in the density of states of the oxygen isotope O(16) at the temperature chosen in Fig. 3 ($T=80$ K), whereas for O(18) the superconducting gap has already completely disappeared.

Note that similar results have been obtained by Schüttler and Pao.[29] They also find that the electron-phonon interaction reduces the critical temperature of spin-fluctuation-induced superconductivity considerably, whereas the isotope exponent remains small but negative. However, in their calculation this is due to the local nature of the electron-phonon interaction whereas the focus of our work is to investigate the role of the k dependence of this interaction.

In order to obtain an estimate for the critical temperature of the two oxygen isotopes, we have performed successive calculations in the temperature range between 78 and 83 K. Since the self-consistent solution of the Eliashberg equations

gives rise to a finite single-particle scattering rate in the gap once the temperature is nonzero we choose the disappearance of the dip structure in the DOS as criterion for T_c. In this way we obtain for the oxygen isotope O(16) a critical temperature of $T_c=82$ K and for the isotope O(18) $T_c=80$ K. Using these values for the calculaion of the isotope exponent $\alpha = -\partial(\ln T_c)/\partial(\ln m) \approx -(\Delta T_c/T_c)(m/\Delta m)$, we obtain an approximate value of $\alpha \approx 0.2$, which is only slightly larger than experimentally found in optimally doped cuprates.
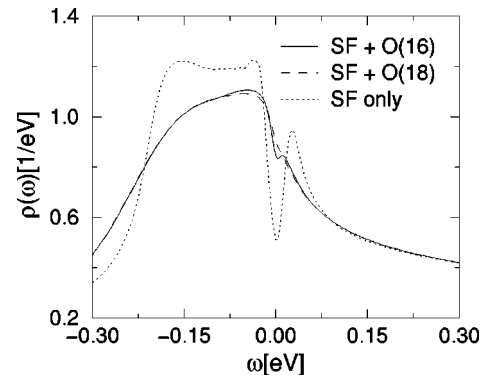

FIG. 3. Momentum-averaged electronic density of states at $T=80$ K for a superconducting state induced only by spin fluctuations and by the spin fluctuation and electron-phonon interaction together for two different different oxygen isotopes O(16) and O(18).
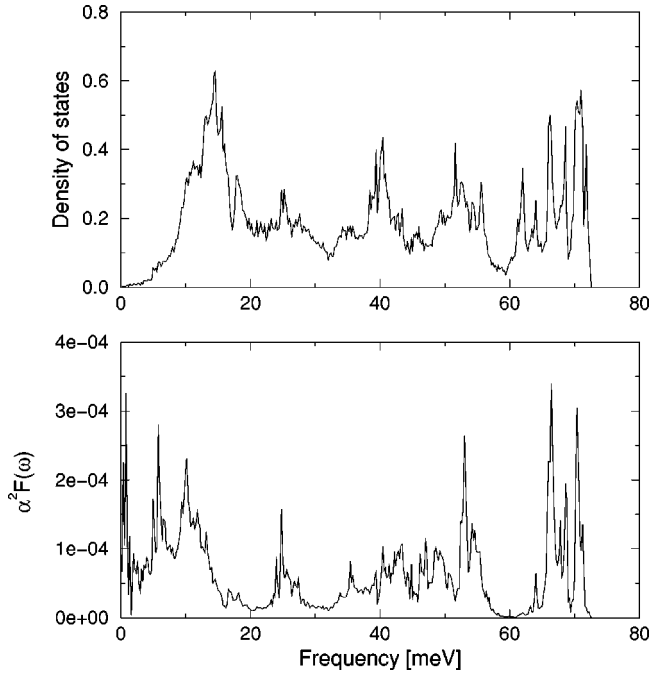
FIG. 4. Phonon density of states for $YBa_2Cu_3O_7$ obtained from a shell-model calculation using parameters as in Ref. 21, and the McMillan function $\alpha^2F(\omega)$. The calculation of the DOS and $\alpha^2F(\omega)$ were performed with a channel width of 0.2 meV.

For a better understanding of the phononic contribution to the pairing interaction and the reason for the positive isotope effect, the phonons will be analyzed separately now. The phonon density-of-states and the McMillan function α^2F are shown in Fig. 4. For total electron-phonon coupling strength we obtain $\lambda=0.47$, which is in good agreement with estimates of $\lambda_{tot}=0.4-0.6$ (Refs. 24 and 25) from experimental determination of frequency shifts and linewidths. Nevertheless, the calculated $\lambda=0.47$ should lead to a considerable contribution to the resistivity, which within the spin-fluctuation model is believed to be dominated by purely electronic scattering. This indicates that the role and relative weight of these two scattering channels for transport phenomena is not yet completely understood. We checked that modifications of λ due to backscattering vertex corrections do not reduce λ considerably.

In Fig. 5(a), we show the momentum dependence of the zero-frequency effective phonon-mediated electron-electron interaction of Eq. (7) . The interaction is attractive for all momenta and most important for the present study peaked for small momentum transfer. In Fig. 5(b), we show the on site interaction V_{00}:

$$V_{00} = \frac{1}{N} \sum_{k_x,k_y} V(k_x,k_y), \qquad (15)$$

which represents the pairing interaction in the case of isotropic s-wave superconductivity, and the nearest-neighbor interaction V_{10}:

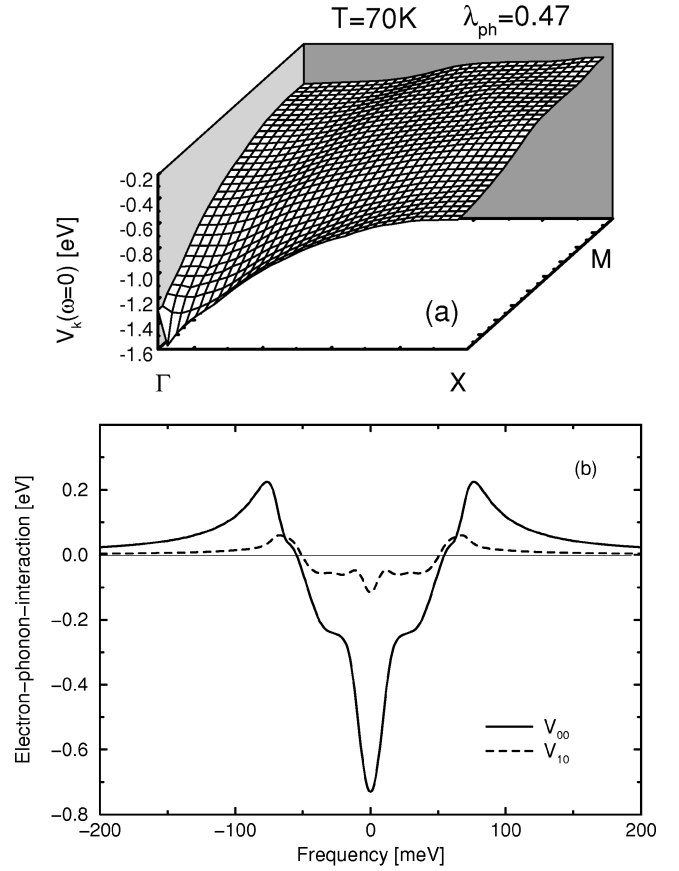$$V_{10} = \frac{1}{N} \sum_{k_x,k_y} V(k_x,k_y)\cos k_x, \qquad (16)$$

FIG. 5. The Electron-phonon interaction at $T=70$ K and $\lambda_{ph}=0.47$: (a) momentum dependence of the electron-phonon interaction V_k for frequency $\omega=0$, (b) frequency dependence of the on-site pairing interaction V_{00} and the nearest-neighbor pairing interaction V_{10}.

which represents the pairing interaction in the case of $d_{x^2-y^2}$-symmetry superconductivity.[26] Both V_{00} and V_{10} are attractive in some frequency range, but the on-site interaction is much stronger and the corresponding attractive frequency range is slightly larger. Therefore, phonons alone will give rise to s-wave superconductivity. This is natural for a phononic mechanism, since the electron-phonon interaction is attractive for all momenta and thus the momentum-averaged interaction V_{00} is dominant. The self-consistent solution of the Eliashberg equations confirms this. Taking only the electron-phonon interaction into account, we obtain superconductivity with anisotropic s-wave symmetry without nodes as can be seen from the momentum dependence of the off-diagonal self-energy in Fig. 6. For obtaining this result at the numerically accessible temperatures $T>30$ K we had to double the total electron-phonon coupling strength artificially. But we expect that enhancing the coupling strength should solely increase the critical temperature and not change the symmetry of the superconducting state. Even for this artificially large coupling strength of $\lambda=0.96$ superconductivity already vanishes between about $T=45-50$ K. Hence, for realistic coupling strengths the critical temperature of phonon-induced superconductivity is much smaller than the critical temperature of spin-fluctuation-induced superconductivity. Note that in this case the repulsive Coulomb interaction was not taken into account, which will suppress
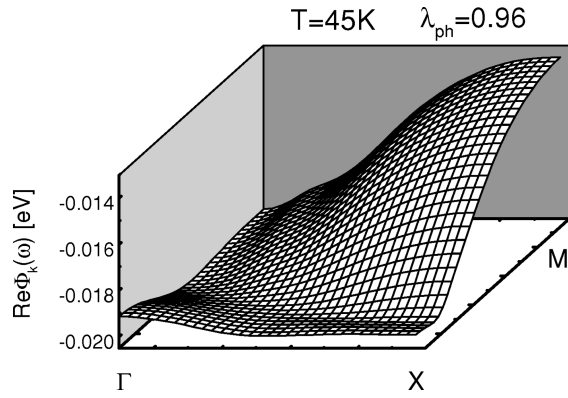
FIG. 6. Off-diagonal self-energy for only phonon-induced superconductivity. The momentum dependence exhibits clearly an anisotropic s-wave symmetry.

the critical temperature of the s-wave superconducting state even more.

Most interesting, however, is the result that all phonon modes together can generate an attractive interaction between nearest-neighbor sites. Thus the consideration of the electron-phonon coupling increases the pairing interaction in the $d_{x^2-y^2}$-wave channel, which is a necessary prerequisite for a positive isotope effect. The reason for the resulting decrease of the superconducting gap due to the presence of phonons is the large on-site interaction V_{00}, which enhances the scattering rate dramatically. Therefore, concerning the sign of the isotope effect, it is plausible, that the isotope effect is positive as long as the positive contribution from the increased pairing interaction V_{10} (where the larger cutoff corresponds to the smaller oxygen mass) outweighs the negative contribution from the increased scattering rate due to larger on-site interaction V_{00}. Also it is clear that including both the spin fluctuation and the electron-phonon interaction still yields $d_{x^2-y^2}$ superconductivity, since the consideration of electron-phonon coupling even increases the $d_{x^2-y^2}$-pairing interaction, whereas the spin-fluctuation contribution to V_{00}, the s-wave pairing interaction, is strongly repulsive, as can be seen from Fig. 1, and therefore reduces the s-wave pairing interaction dramatically.

We will focus now on why the nearest-neighbor electron-phonon interaction is attractive at all. The attractiveness of V_{10} can be traced back to the fact that the phononic interaction is peaked for small momentum transfer, since multiplication with $\cos k_x$ in Eq. (16) gives more weight to small
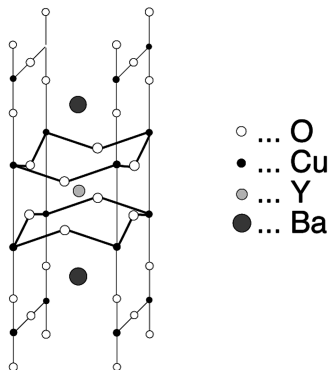

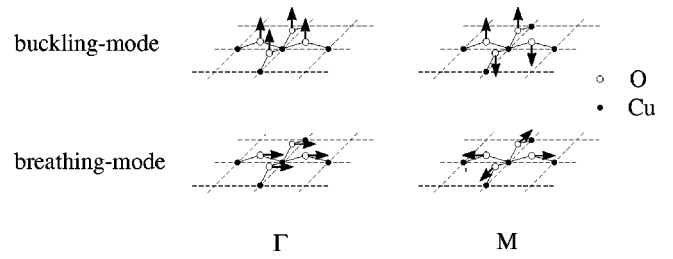FIG. 7. Structure of $YBa_2Cu_3O_7$.

FIG. 8. Displacement patterns of the buckling mode and of the breathing mode at the Γ point and the M point of the BZ.

momenta. Obviously, besides the shape of the Fermi surface, which is taken from angle-resolved photoemission spectroscopy experiments, the momentum dependence of the electron-phonon interaction is the key feature, which controls possible contributions to different pairing symmetries. The momentum dependence of the electron-phonon interaction consists of two contributions, as can be seen by inspection of Eq. (7); namely the momentum dependence of the electron-phonon coupling constants and the momentum dependence of the phonon-Green's function. Because the momentum dependence of the phonon-Green's function is directly related to the dispersion of the phonon spectrum, which is relatively weak in the case of dominating optical phonon modes, we find that the momentum dependence of the electron-phonon coupling constants is the decisive factor. Therefore, phonon modes with coupling strength largest for small momentum transfer can enhance the $d_{x^2-y^2}$-pairing interaction. However, phonon modes with coupling strongest for large momentum transfer reduce the $d_{x^2-y^2}$-pairing interaction.

In order to find out which phonon modes support the $d_{x^2-y^2}$-pairing interaction, the vibrations of single atoms (per unit cell) will be investigated. For an illustration of the structure of $YBa_2Cu_3O_7$ we refer to Fig. 7. The greatest coupling strength is caused by the vibration of the in-plane oxygens O(II), with vibration amplitudes along the Cu-O bonding axis and along the z axis, i.e., breathing-mode-like and buckling-mode-like vibrations, and by the vibrations of the apex oxygen O(I) in the z direction. For illustration of the displacement patterns of the breathing mode and the buckling mode we refer to Fig. 8. In Fig. 9 the momentum dependence along the $\Gamma \rightarrow M$ direction of the corresponding electron-phonon coupling is shown. The in-plane oxygen O(II,III) vibrations are quite well described by the momentum dependence $g(\mathbf{k}) \sim (\sin k_x + \sin k_y)$ and $g(\mathbf{k}) \sim (\cos k_x + \cos k_y)$, which is the result for the breathing and buckling mode, respectively, if only nearest-neighbor interaction is considered. Thus the breathing mode reduces $d_{x^2-y^2}$ superconductivity, because the momentum dependence of its coupling strength is peaked for large momentum transfer. On the other hand, the coupling strength of the buckling mode is peaked for small momentum transfer and therefore the buckling mode supports $d_{x^2-y^2}$-wave superconductivity in so far as the $d_{x^2-y^2}$-pairing interaction is increased by the buckling mode. The small wiggles in Fig. 9 are caused by wiggles in the momentum dependence of the free susceptibility $\chi_{\mathbf{q}}^0$, which determines the screening properties of the CuO_2 planes (see the Appendix). In the case of the apex oxygen vibrations, the momentum dependence of the coupling is dif-
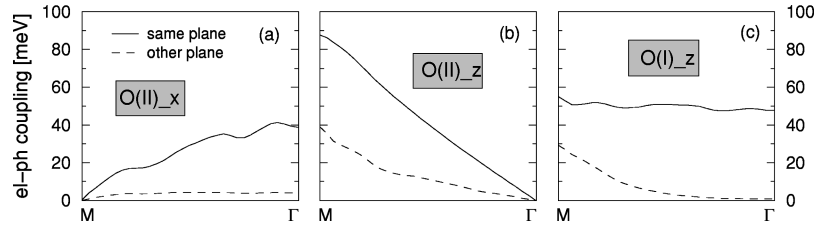
FIG. 9. Electron-phonon coupling constant for the vibration of the in-plane oxygen O(II) (a) in the x direction, (b) in the z direction, and (c) for the vibration of the apex oxygen O(I) in the z direction. Since every hole is located just in one of the planes, the coupling is different for the vibrations of the oxygens of the two planes. The coupling of the oxygen in the same plane is denoted by a solid line and the coupling of the oxygen of the other plane by a dashed line. Note, in the case of the apex oxygen, this refers to the closer and the further apex oxygen.

ferent for the two apex ions in the primitive cell: the closer apex oxygen causes a more or less momentum-independent coupling, whereas the coupling of the further apex oxygen is stronger for small momentum transfer similar to the buckling-mode-like vibrations. In respect to vibrations of the other ions, which are not shown in Fig. 9, we find that the coupling of vibrations in the z direction is generally peaked for small momentum transfer. The vibration of the oxygen ions is the most dominant contribution to the total coupling strength, whereas the contribution of yttrium and barium is very small due to screening in the CuO_2 planes. Altogether all vibrations in the z direction, especially the buckling modes, increase the nearest-neighbor interaction V_{10}. Only the breathing mode and the vibration of the chain oxygen O(IV) along the CuO-bonding axis reduce V_{10}. The other modes are of no relevance with respect to V_{10}.

Note that within our approach the coupling strength of the buckling mode is about twice as large as the coupling strength of the breathing mode. The situation is opposite, if the same calculations are performed with the original Zeyher model. The reason for this is to be found in the different treatment of screening. In Zeyher's model the screening planes are smeared over the whole elementary cell, whereas in our approach the exact position of the CuO_2 planes with respect to the vibrating ion and the Cooper-pairing hole is considered. It is evident that the screening of the breathing mode is better, if one accounts for the fact that both the vibrating oxygen ion and the Cooper pair-forming hole are located within the same plane. On the other hand the opposite is true for the buckling mode. Because the vibration of the oxygen ion in the z direction is perpendicular to the CuO_2 plane, it cannot be screened within the same plane, but only by charges induced in more distant planes. Therefore, the buckling mode is less screened, if one takes the relative location of the vibrating oxygen ion, the Cooper-pairing hole, and the screening plane explicitly into account. Additionally, it has to be pointed out that in our approach (as in the Zeyher model) only the electrostatic part of the electron-phonon coupling is considered, whereas all contributions arising from changes in the overlap of neighboring electronic wave functions have been neglected. It is to be expected that these neglected effects are strongest for the breathing mode. This means that the coupling strength of the breathing mode could be somewhat underestimated in our approach. In this respect it is interesting to note that recently the electron-phonon coupling was calculated by Andersen *et al.*[27] and Jepsen *et al.*[28] within a tight-binding model derived from local-density approximation linear-response calculations. They find a total electron-phonon coupling strength of $\lambda_s \approx 0.4$, which is similar to our findings, and a medium $d_{x^2-y^2}$-wave coupling strength of $\lambda_d \approx 0.3$, which is even much larger than our value. Most interesting, they also find a very dominant coupling of the buckling mode. Although their approach is complementary to ours, their results are quite similar, which supports our results concerning the relative coupling strengths of the breathing and the buckling mode. Anyway we expect that a more dominant breathing mode would reduce V_{10} somewhat, leaving the other results qualitatively unchanged.

Our numerical results, obtained within a strong-coupling Eliashberg theory, show that the electron-phonon interaction reduces the critical temperature, even though it increases the d-wave pairing interaction and the isotope effect is positive. In order to investigate these aspects in a qualitative, but more transparent way, we use a simple weak-coupling model, where the pairing interactions caused by spin fluctuations and phonons are approximated by frequency-independent coupling constants λ_{sf}^d and λ_{ph}^d with different cutoffs ω_{sf} and ω_{ph} (Fig. 10). Introduction of the renormalization constants $Z_{sf}=1+\lambda_{sf}$ and $Z_{sf-ph}=1+\lambda_{sf}+\lambda_{ph}$ accounts for the reduction of the spectral weight of the Cooper pair-forming holes by scattering effects due to spin fluctuations and phonons. For the renormalization factors the same cutoff is used as for the pairing interaction. The coupling constants λ are defined in Eq. (8). The coupling constant λ^d characterize the $d_{x^2-y^2}$-pairing interaction:
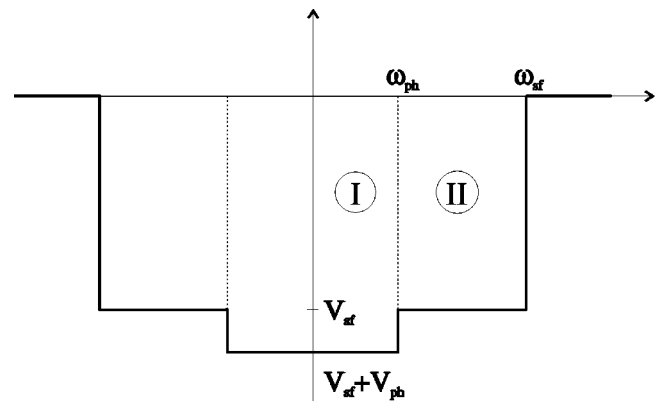

FIG. 10. Modeling of the spin-fluctuation interaction and the electron-phonon interaction by frequency independent coupling constants. Here, $V_{sf}=\lambda_{sf}^d$ and $V_{ph}=\lambda_{ph}^d$ denote the $d_{x^2-y^2}$-type contribution of the corresponding interactions, respectively, with cutoff ω_{sf} and ω_{ph}.
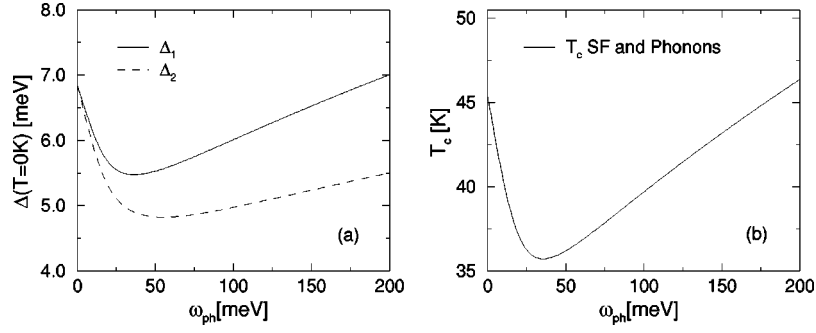
FIG. 11. Results for Δ and T_c using the simplified interaction model taking $\omega_{sf} = 200$ meV, $\lambda_{sf}^d = 1.1$, $\lambda_{sf} = 3.2$, $\lambda_{ph}^d = 0.3$, $\lambda_{ph} = 0.6$.

$$\lambda^d = \frac{\sum_{\mathbf{kk'}} \delta(\epsilon_{\mathbf{k}}) \delta(\epsilon_{\mathbf{k'}}) \mathrm{Re} V(\mathbf{k},\mathbf{k'},0) \psi_{\mathbf{k}}^d \psi_{\mathbf{k'}}^d}{\sum_{\mathbf{kk'}} \delta(\epsilon_{\mathbf{k}}) \delta(\epsilon_{\mathbf{k'}}) \psi_{\mathbf{k}}^d \psi_{\mathbf{k'}}^d} \quad (17)$$

with $\psi_{\mathbf{k}}^d = \cos k_x - \cos k_y$. These approximations result in the following form of the gap-function $\Delta_{\mathbf{k}} = \Delta_0 \psi_{\mathbf{k}}^d$ with $\Delta_0 = \Delta_1$ if $|\epsilon_{\mathbf{k}}| < \omega_{ph}$ and $\Delta_0 = \Delta_2$ if $\omega_{ph} < |\epsilon_{\mathbf{k}}| < \omega_{sf}$, respectively. Δ_1, Δ_2 are obtained by solving the gap equations:

$$\Delta_1 = \frac{\lambda_{sf}^d + \lambda_{ph}^d}{z_{sf\text{-}ph}^2} \int_0^{\omega_{ph}} d\epsilon \frac{1 - 2f(\epsilon_1)}{\epsilon_1} \Delta_1$$

$$+ \frac{\lambda_{sf}^d}{z_{sf}^2} \int_{\omega_{ph}}^{\omega_{sf}} d\epsilon \frac{1 - 2f(\epsilon_2)}{\epsilon_2} \Delta_2 \quad (18)$$

and

$$\Delta_2 = \frac{\lambda_{sf}^d}{z_{sf\text{-}ph}^2} \int_0^{\omega_{ph}} d\epsilon \frac{1 - 2f(\epsilon_1)}{\epsilon_1} \Delta_1 + \frac{\lambda_{sf}^d}{z_{sf}^2} \int_{\omega_{ph}}^{\omega_{sf}} d\epsilon \frac{1 - 2f(\epsilon_2)}{\epsilon_2} \Delta_2. \quad (19)$$

with

$$\epsilon_1 = \sqrt{\frac{\epsilon^2}{z_{sf\text{-}ph}^2} + \Delta_1^2}, \quad \epsilon_2 = \sqrt{\frac{\epsilon^2}{z_{sf}^2} + \Delta_2^2}. \quad (20)$$

In the following we will study the influence of the size of the phonon cutoff ω_{ph} on the superconducting properties by means of this simple model. In Fig. 11(a) the gap functions Δ_1 and Δ_2 corresponding to the regions I ($|\epsilon_{\mathbf{k}}| < \omega_{ph}$) and II ($\omega_{ph} < |\epsilon_{\mathbf{k}}| < \omega_{sf}$) at $T = 0$ K are plotted and in Fig. 11(b) the corresponding critical temperature is shown. The coupling constants $\lambda_{sf}, \lambda_{sf}^d, \lambda_{ph}, \lambda_{ph}^d$ are chosen in agreement with the previous results. Only λ_{ph}^d is chosen slightly larger for illustrational purposes. Since the spin-fluctuation interaction is decreasing slowly over a large frequency range, as can be seen by inspection of Fig. 1, it is hard to estimate the spin-fluctuation cutoff ω_{sf}. In this calculation $\omega_{sf} = 200$ meV was chosen as a cutoff. Two things can be observed in Fig. 11: First, the gap function Δ_1 (region I) is generally larger than the gap function Δ_2 (region II) due to an increased pairing interaction caused by the phonons. Furthermore the gap functions Δ_1 and Δ_2 and the critical temperature T_c show a peculiar ω_{ph} dependence: for small ω_{ph} they are decreasing as a function of ω_{ph} and after a certain

critical cutoff frequency they are increasing again. Examination of gap equation Eq. (19) shows that there are two contributions, which determine the size of the gap function Δ_1: the interaction of charge carriers (I) among themselves and the interaction of charge carriers (I) with charge carriers (II). In an analogous manner there are two contributions, which determine the size of the gap function Δ_2. Only one of these (four) contributions, i.e., both electrons in region I, can profit from the phononic part of the pairing interaction. On the other hand, two of these (four) contributions, each of which result from the interaction of the respective electrons with electrons of region I, are reduced, because the quasiparticle spectral weight in region I is diminished by the additional scattering on phonons. Altogether only the gap function Δ_1 can profit from the phononic contribution to the pairing interaction, whereas both gap functions Δ_1 and Δ_2 notice the destructive effect due to scattering on phonons. This is the reason why for small ω_{ph} both of the gap functions Δ_1 and Δ_2 are decreasing as a function of ω_{ph}. In the larger region I more electrons are scattered by phonons. Only when region I has become large enough and ω_{ph} exceeds a critical cutoff frequency, does the positive effect of increased pairing interaction between Cooper pairs in region I outweigh the negative effect of additional scattering, and thus both gap functions Δ_1 and Δ_2 start increasing as a function of ω_{ph} for larger frequencies.

The ω_{ph} dependence of T_c shown in Fig. 11(b) displays an analogous behavior. For very small ω_{ph} the critical temperature is decreasing, and after passing through a minimum, T_c is increasing again yielding a positive isotope effect. The critical temperature itself will, for realistic phonon frequencies ω_{ph}, be smaller than the critical temperature of only spin-fluctuation-induced superconductivity.

From Fig. 11(b) we can directly extract the isotope exponent. For very small phonon frequencies the critical temperature is decreasing for increasing ω_{ph}. Hence, the isotope exponent α is negative in this region. For larger ω_{ph}, after passing through a minimum, T_c is increasing with ω_{ph}. This causes a positive isotope exponent. The magnitude of α depends on the relative size of the coupling strengths of the electron-phonon and spin-fluctuation interaction and the corresponding scattering rates. In Fig. 12 the isotope exponent vs λ_{sf}^d and λ_{sf} is shown for different values of λ_{ph}^d. For decreasing spin-fluctuation contribution λ_{sf}^d to the pairing interaction the isotope exponent is increasing strongly. This is obvious, because the electron-phonon coupling becomes the
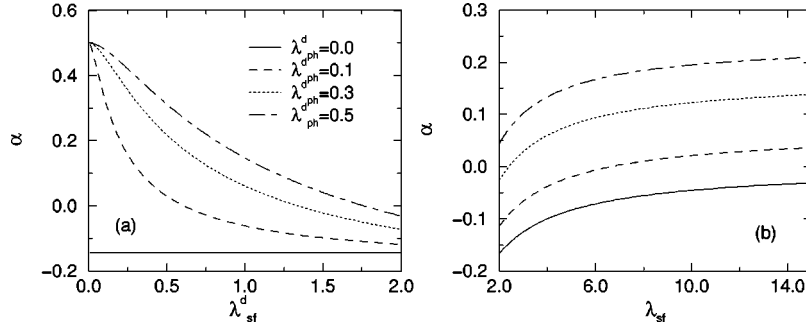
FIG. 12. Dependence of the isotope exponent α on the spin-fluctuation $d_{x^2-y^2}$-coupling strength and the total spin-fluctuation coupling strength, respectively. These results were obtained with the simple weak-coupling model with $\omega_{sf}=200$ meV, $\omega_{ph}=70$ meV, and additionally (a) $\lambda_{sf}=2.5$ and (b) $\lambda_{sf}^d=1.3$, respectively. The total electron-phonon coupling strength was taken as $\lambda_{ph}=1$, but the $d_{x^2-y^2}$-electron-phonon coupling strength was varied as indicated in the figure.

origin for superconductivity, a situation which seems unlikely for cuprates due to the large phononic coupling constants necessary in this case.

The isotope exponent of the present work is always small in magnitude and positive. For the system $YBa_2Cu_3O_7$, under consideration, this is in qualitative agreement with the experimental observation. Whether the increase of α for nonoptimal doping concentration is solely due to the decreasing strength of the leading electronic pairing interaction or of a more subtle nature is beyond the scope of the present paper.

IV. SUMMARY

In summary, we find that spin-fluctuation-induced $d_{x^2-y^2}$ superconductivity is robust against the existence of electron-phonon coupling. The superconducting transition temperature is reduced by the interaction with phonons due to an enhancement of the electron-scattering rate. Furthermore, we find that the momentum dependence of the electron-phonon interaction increases the $d_{x^2-y^2}$-pairing interaction slightly. This is important for getting a positive isotope effect. Our results indicate that the isotope effect is small for optimal doping. If one assumes that the spin-fluctuation coupling strength varies with the doping concentration, this would imply a strong doping dependence of the isotope effect.

A major approximation of the present work is the neglect of the effect of strong electronic correlation on the electron-phonon coupling constants. As shown by Lichtenstein and Kulić[30] strong electronic correlation cause a suppression of charge fluctuations at small distances. Therefore, we expect $g_\lambda(\mathbf{k})$ to be reduced for zone-boundary phonons. This would decrease λ_{ph}^s and thus the large scattering rate due to phonons. For the same reason, we expect λ_{ph}^d to be slightly enhanced by electronic correlations.

Our results demonstrate that the existence and sign of the isotope effect can be understood within a spin-fluctuation-induced d-wave state. Due to the d-wave nature of the superconducting state, it is particularly important to obtain a proper description of the momentum dependence of the electron-phonon interaction. It was shown that out-of-plane vibrations are essential for the d-wave state and that one cannot focus solely on one particular phononic mode. Finally, the strong electronic correlations inhibit the occur-

rence of a phonon-induced superconducting state with s-wave symmetry. A phonon-induced d-wave state can be excluded because of the insufficient strength of this subdominant pairing interaction.

APPENDIX: DERIVATION OF THE INVERSE DIELECTRIC FUNCTION

In this appendix the treatment of the local field corrections arising from the position of the screening CuO_2 planes relative to the vibrating ion will be discussed. If spatial inhomogeneity is taken into account, the dielectric function becomes a matrix in the reciprocal-lattice vectors $\mathbf{G},\mathbf{G}'$:

$$\epsilon(\mathbf{k}+\mathbf{G},\mathbf{k}+\mathbf{G}')=\epsilon_\infty\delta_{\mathbf{G}\mathbf{G}'}-v(\mathbf{k}+\mathbf{G})\tilde{\chi}(\mathbf{k}+\mathbf{G},\mathbf{k}+\mathbf{G}').$$
(A1)

Here, $\tilde{\chi}$ is the irreducible polarization of the density-density correlation function χ, which characterizes the screening properties of the system. The inverse dielectric function is defined by

$$\sum_{\mathbf{G}''}\epsilon(\mathbf{k}+\mathbf{G},\mathbf{k}+\mathbf{G}'')\epsilon^{-1}(\mathbf{k}+\mathbf{G}'',\mathbf{k}+\mathbf{G}')=\delta_{\mathbf{G}\mathbf{G}'}.$$
(A2)

This can be expressed as

$$\epsilon^{-1}(\mathbf{k}+\mathbf{G},\mathbf{k}+\mathbf{G}')=\frac{1}{\epsilon_\infty}[\delta_{\mathbf{G}\mathbf{G}'}+v(\mathbf{k}+\mathbf{G})\chi(\mathbf{k}+\mathbf{G},\mathbf{k}+\mathbf{G}')].$$
(A3)

The susceptibility χ has to be determined by solving the following integral equation:

$$\epsilon_\infty\chi(\mathbf{k}+\mathbf{G},\mathbf{k}+\mathbf{G}')$$
$$=\tilde{\chi}(\mathbf{k}+\mathbf{G},\mathbf{k}+\mathbf{G}')+\sum_{\mathbf{G}''}\tilde{\chi}(\mathbf{k}+\mathbf{G},\mathbf{k}+\mathbf{G}'')$$
$$\times v(\mathbf{k}+\mathbf{G}'')\chi(\mathbf{k}+\mathbf{G}'',\mathbf{k}+\mathbf{G}').$$
(A4)

In the cuprates the most dominant screening is caused by mobile charges within the CuO_2 planes. In $YBa_2Cu_3O_7$ there are two planes per unit cell. Therefore, the susceptibility χ is a 2×2 matrix, describing density-density correlations within the same plane and between both of the planes. The polarization $\widetilde{\chi}$, on the other hand, reduces to a diagonal matrix, because the particles are assumed to be confined to the planes. In real space the polarization is given by

$$\widetilde{\chi}(\mathbf{r_1},\mathbf{r_2}) = \widetilde{\chi}^{2D}(\mathbf{x_1}-\mathbf{x_2})\,\delta(z_1-z_2)\sum_{j\beta}\ \delta(z_1-z_{j\beta}), \quad (A5)$$

where $z_{j\beta}=jc+d_\beta$ are the z coordinates of the CuO_2 planes, with j being the index for the primitive cell, β is the index for the CuO_2 plane within the primitive cell, and c is the height of the primitive cell. Fourier transformation yields

$$\widetilde{\chi}(\mathbf{k+G},q+Q,q+Q') = \frac{1}{c}\widetilde{\chi}^{2D}(\mathbf{k+G})\sum_\beta\ e^{i(Q-Q')d_\beta}.$$
$$(A6)$$

Here, $\mathbf{k},\mathbf{G}$ refer to the in-plane wave vectors, whereas q,Q represent the wave vectors in the z direction. In the random-phase approximation $\widetilde{\chi}^{2D}$ reduces to the noninteracting particle-hole bubble of the holes in the CuO_2 planes. $\widetilde{\chi}$ is diagonal with respect to the in-plane wave vectors and the Q dependence is simple enough. This permits an analytic treatment of the Q summations. Therefore, Eq. (A4) can be inverted easily and the inverse dielectric function can be obtained in this way. There remains only the question of how to choose the z coordinate d_β of the screening planes, which are not unambiguous due to the internal buckling of the CuO_2 planes. In our calculations we assumed that the screening plane should follow the buckling of the CuO_2 plane.

---

*Present address: Institut für Theorie der Kondensierten Materie, Universität Karlsruhe, D-76128 Karlsruhe, Germany.

[1] P. Monthoux, A. Balatsky, and D. Pines, Phys. Rev. Lett. **67**, 3448 (1991).

[2] T. Moriya, K. Ueda, and Y. Takahashi, J. Phys. Soc. Jpn. **49**, 2905 (1990).

[3] N. E. Bickers, D. J. Scalapino, and R. T. Scalettar, Int. J. Mod. Phys. B **1**, 687 (1987).

[4] A. J. Millis, H. Monien, and D. Pines, Phys. Rev. B **42**, 167 (1990); V. Barzykin and D. Pines, *ibid.* **52**, 13 585 (1995).

[5] (a) B. P. Stojković and D. Pines, Phys. Rev. Lett. **76**, 811 (1996); (b) Phys. Rev. B **55**, 8576 (1997).

[6] J. Schmalian, D. Pines, and B. P. Stojković, Phys. Rev. Lett. **80**, 3839 (1998).

[7] A. V. Chubukov and J. Schmalian, Phys. Rev. B **57**, R11 085 (1998).

[8] P. Monthoux and D. Pines, Phys. Rev. B **49**, 4261 (1994).

[9] R. Feile, Physica C **159**, 1 (1989).

[10] A. P. Litvinchuk, C. Thomsen, and M. Cardona, in *Physical Properties of High-T$_c$ Superconductors IV*, edited by D. M. Ginsberg (World Scientific, Singapore, 1994), p. 375.

[11] R. M. Macfarlane, Hal Rosen, and H. Seki, Solid State Commun. **63**, 831 (1987).

[12] A. P. Litvinchuk, C. Thomsen, and M. Cardona, Solid State Commun. **83**, 343 (1992).

[13] J. P. Franck, in *Physical Properties of High-T$_c$ Superconductors IV* (Ref. 10), p. 189.

[14] A. Nazarenko and E. Dagotto, Phys. Rev. B **53**, R2987 (1996).

[15] T. Dahm, D. Manske, D. Fay, and L. Tewordt, Phys. Rev. B **54**, 12 006 (1996).

[16] N. Bulut and D. J. Scalapino, Phys. Rev. B **54**, 14 971 (1996).

[17] R. Zeyher and M. L. Kulić, Phys. Rev. B **53**, 2850 (1996).

[18] N. E. Bickers and D. J. Scalapino, Ann. Phys. (N.Y.) **193**, 206 (1989).

[19] F. C. Zhang and T. M. Rice, Phys. Rev. B **37**, 3759 (1988).

[20] W. Cochran, in *Phonons in Perfect Lattices and in Lattices with Point Imperfections*, edited by R. W. H. Stevenson (Oliver & Boyd, Edinburgh, 1966).

[21] J. Humlicek, A. P. Litvinchuk, W. Kress, B. Lederle, C. Thomson, M. Cardona, H.-U. Habermeier, I. E. Trofimov, and W. König, Physica C **206**, 345 (1993).

[22] R. Zeyher, Z. Phys. B **80**, 187 (1990).

[23] J. Schmalian, M. Langer, S. Grabowski, and K. H. Bennemann, Comput. Phys. Commun. **93**, 141 (1996).

[24] A. P. Litvinchuk, C. Thomsen, and M. Cardona, Solid State Commun. **80**, 257 (1991).

[25] B. Friedl, C. Thomsen, and M. Cardona, Phys. Rev. Lett. **65**, 915 (1990).

[26] $V_{10}(\omega)$ may also induce an anisotropic s-wave state like $\Delta_\mathbf{k} \propto (\cos k_x + \cos k_y)$, but the Fermi surface geometry of the cuprates always favors the $d_{x^2-y^2}$ state due to larger gain of condensation energy on the Fermi surface in the $d_{x^2-y^2}$-wave case.

[27] O. K. Andersen, S. Y. Savrasov, O. Jepsen, and A. I. Liechtenstein, J. Low Temp. Phys. **105**, 285 (1996).

[28] O. Jepsen, O. K. Andersen, I. Dasgupta, and S. Savrasov, J. Phys. Chem. Solids **59**, 1718 (1998).

[29] H.-B. Schüttler and C.-H. Pao, Phys. Rev. Lett. **75**, 4504 (1995); Phys. Rev. B **57**, 5051 (1998); J. Supercond. **8**, 633 (1995); J. Phys. Chem. Solids **56**, 1745 (1995).

[30] A. I. Lichtenstein and M. L. Kulić, Physica C **245**, 186 (1995).